Supplement to: Improving the Representation of Aggregation in a Two-moment Microphysical Scheme with Statistics of Multi-frequency Doppler Radar Observations

Markus Karrer[a], Axel Seifert[b], Davide Ori[a], and Stefan Kneifel[a]

[a]Institute for Geophysics and Meteorology, University of Cologne, Cologne, Germany
[b]Deutscher Wetterdienst, Offenbach, Germany

Correspondence: Markus Karrer (markus.karrer@uni-koeln.de)

1 Introduction

Here we provide additional figures, which give additional insight but are not necessary to draw the conclusions of the main text.

Hydrometeor Contents from the ICON-LEM Case Study

The Fig. S1 to S11 show the hydrometeor content in a time-height series of all sensitivity runs presented in Sect. 3.3 in the main text. These time-height series show similar signatures discussed in the idealized profile (Sect. 3.2 in the main text). These are e.g. the faster increase of snow mass and number in the “colMix2_Akernel" (“NEW") run at upper heights (lower temperatures) compared to the default simulation, the faster increase of the mean mass of snow at around -15$^{\circ}C$ and the lower mean mass of snow close to the melting layer. Also the sensitivity runs exhibits signatures, which one could expect from the idealized simulations. These are e.g. the different increase of the mean mass between “colMix2_Akernel" (“NEW") and “colMix2_Akernel_LinCot". However, as suspected in the main text some differences are overestimated in the idealized setup. E.g. the relatively strong difference in the snow mass between “colMix2_Akernel" (“NEW") and “colMix2_Akernel_LinCot" is not present. In these simulation the supersaturation are realistic and consumed by depositional growth, which lead to a more realistic representation of the mass-uptake.

DWRkw Time-height Series of the Case Study

In contrast to DWR$_{X,Ka}$, we can infer from DWR$_{X,Ka}$ (Fig. S12) information about smaller aggregates present mostly at colder temperatures and the size of the rain droplets (which are more compact and therefore smaller than an ice particle of the same mass). DWR$_{Ka,W}$ increases too fast at temperatures about -15 $^{\circ}$C in “colMix2_Dkernel and “colMix2broad_Akernel". This overestimation undermines the importance of the formulation of the aggregation kernel and the broadness of the distribution to match DWR$_{Ka,W}$ accurately. While the different sticking efficiency significantly impacts the simulated DWR$_{Ka,W}$ in the 1D simulations (Fig. 7 of the main text), the difference in the forward operated ICON-LEM simulation appears relatively small. In the ICON-LEM simulation, the weaker growth of the particles in “colMix2_Akernel_LinCot" at colder temperatures might be partly compensated by advection or nucleation.

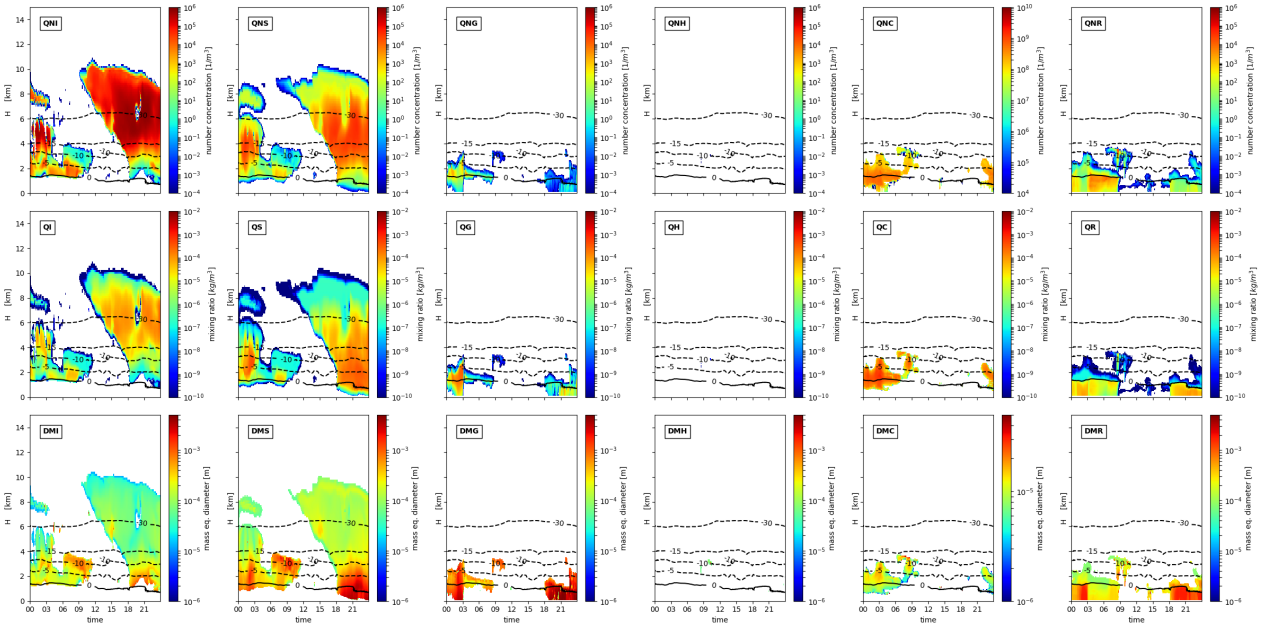

Figure S1. Hydrometeor contents (top: number concentration; middle: mixing ratio; bottom: mass equivalent diameter) of all six categories (I: cloud ice; S: snow; G: graupel; H: hail; C: cloud droplets; R: rain) of the 3rd January 2016 of the default simulation.

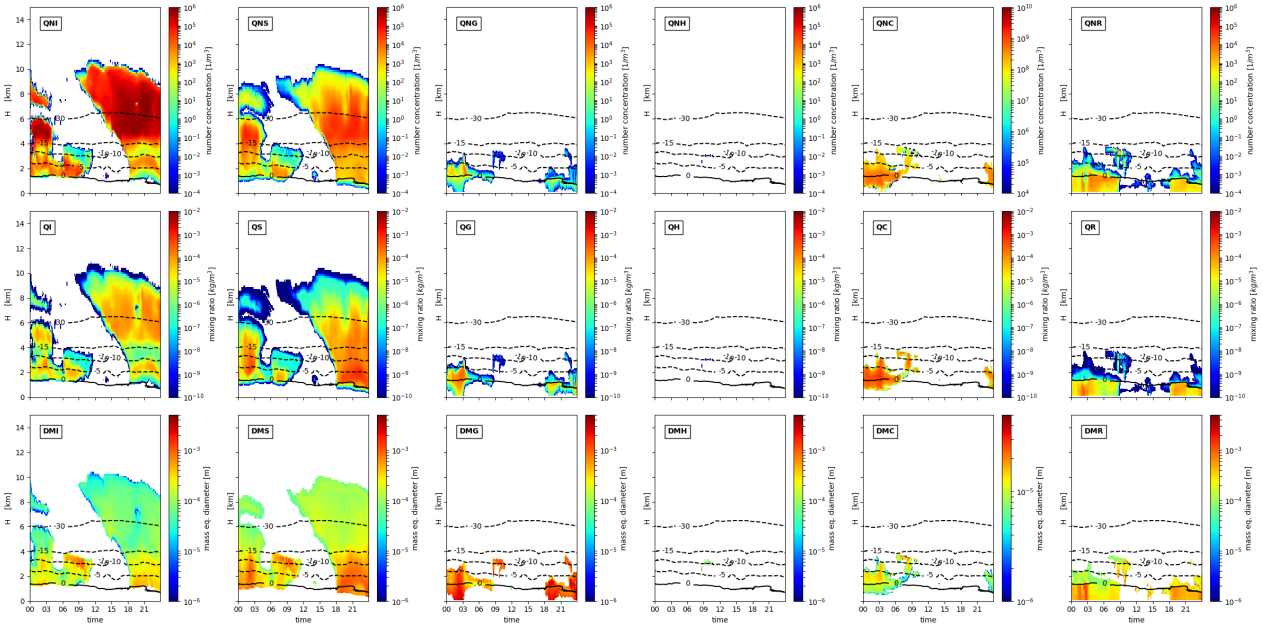

Figure S2. Same as Fig. S1 but for the “colMix2_Akernel" (“NEW") run.

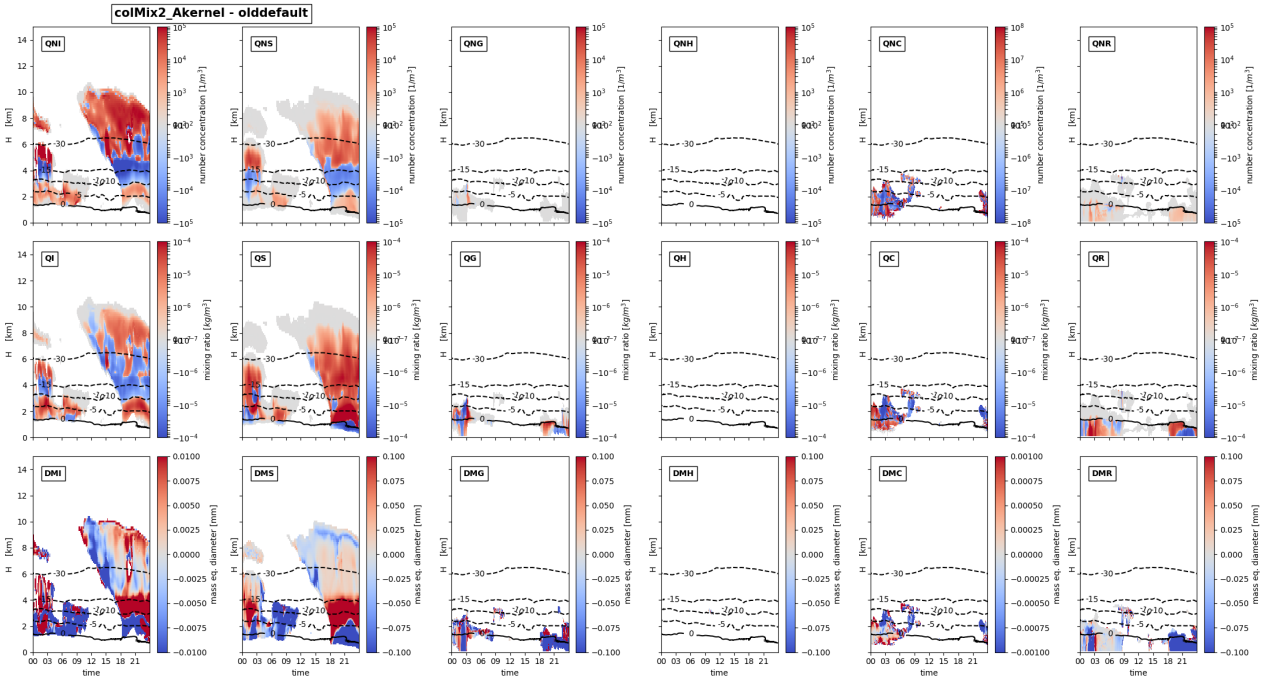

Figure S3. Difference of the hydrometers (same panels as in Fig. S1) between the the “colMix2_Akernel" (“NEW") and the default run.

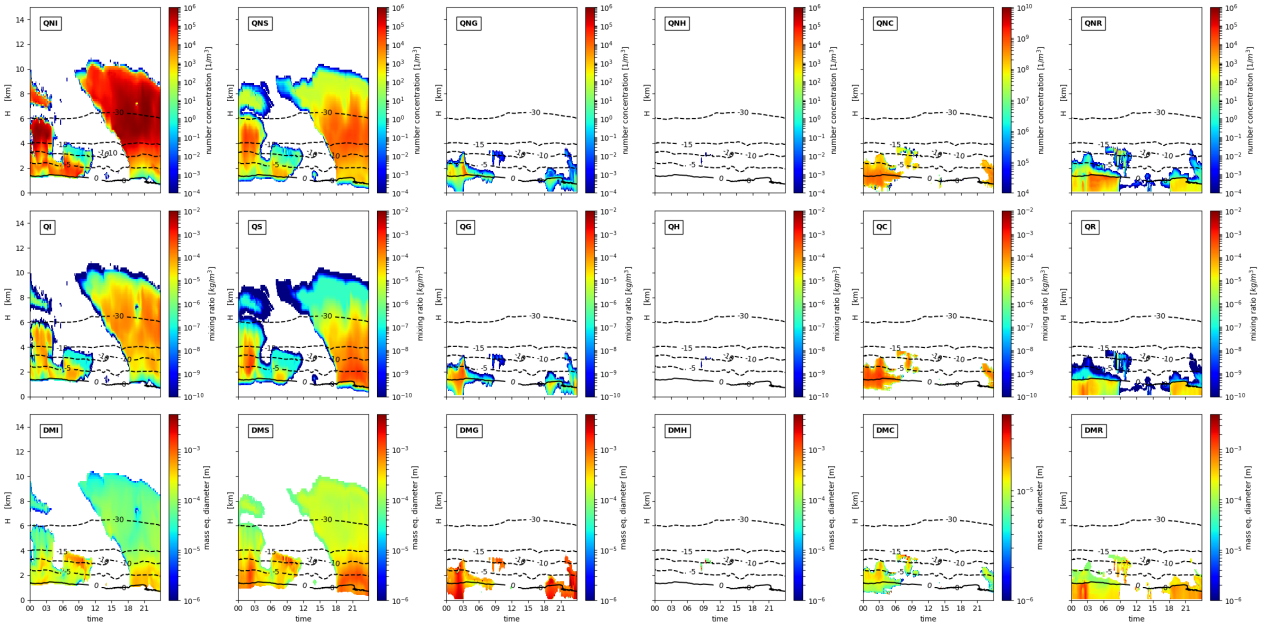

Figure S4. Same as Fig. S1 but for the “colMix2_Akernel_LinCot" run.

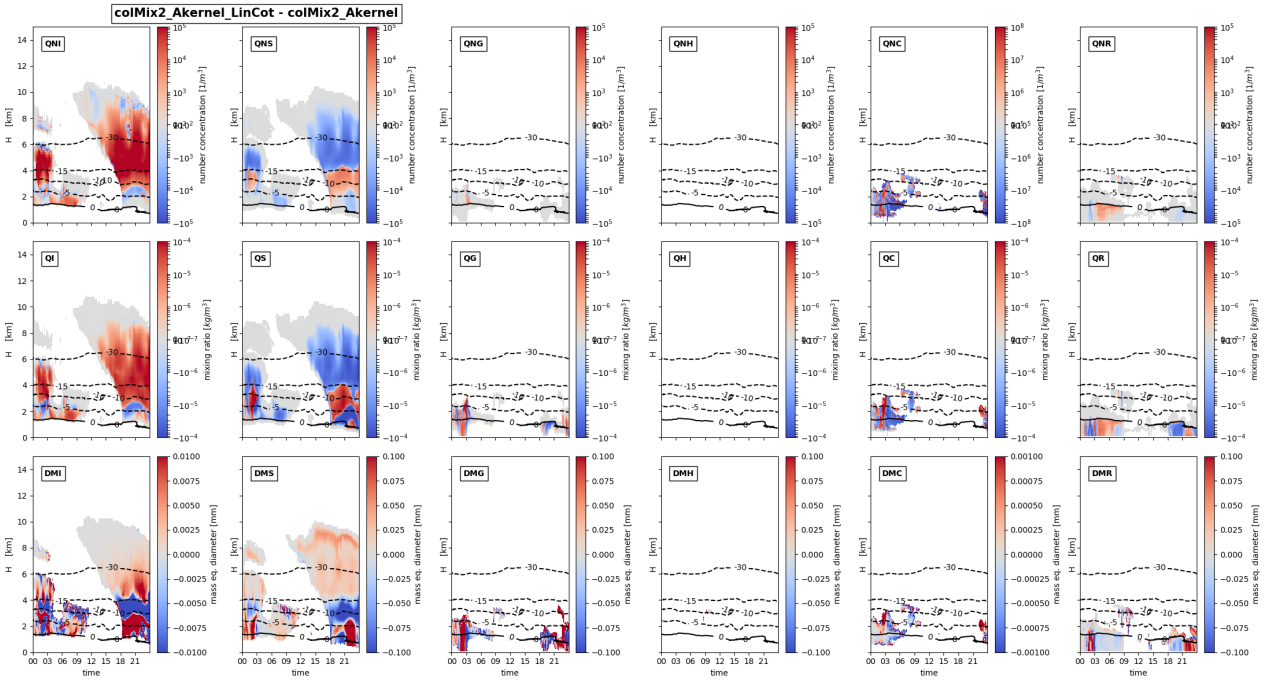

Figure S5. Difference of the hydrometers (same panels as in Fig. S1) between the the "colMix2_Akernel_LinCot" and the "colMix2_Akernel" ("NEW") run.

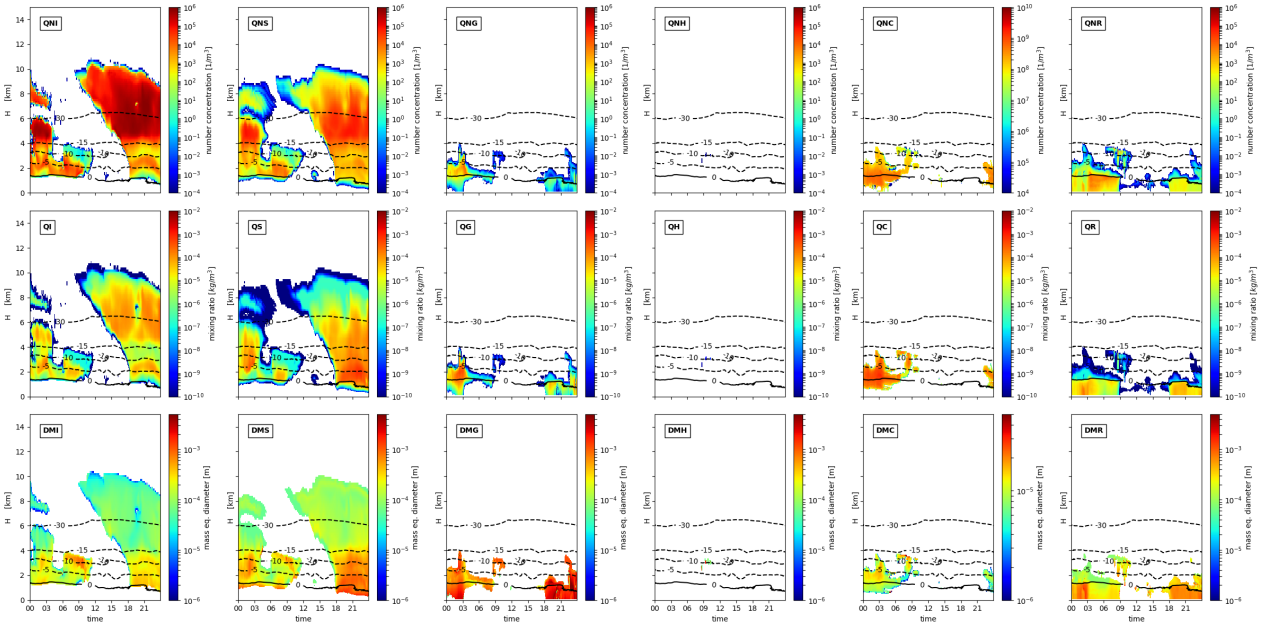

Figure S6. Same as Fig. S1 but for the "colMix2broad_Akernel" run.

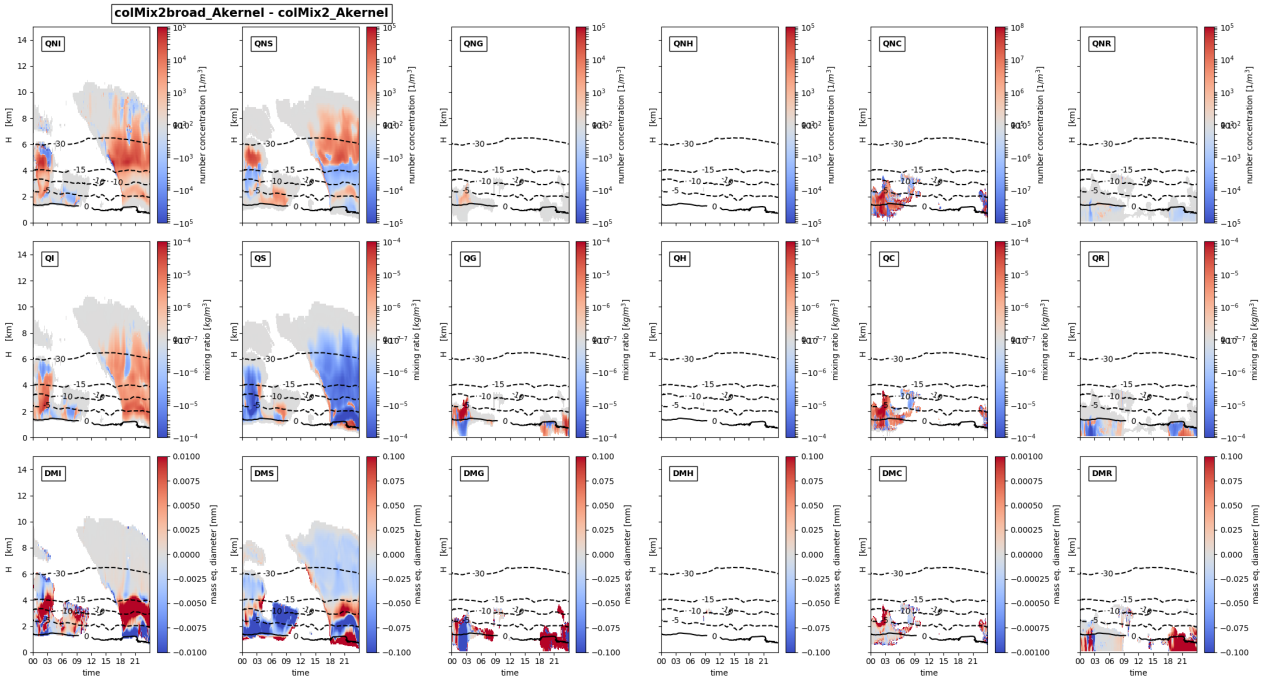

Figure S7. Difference of the hydrometers (same panels as in Fig. S1) between the the “colMix2broad_Akernel" and the “colMix2_Akernel" (“NEW") run.

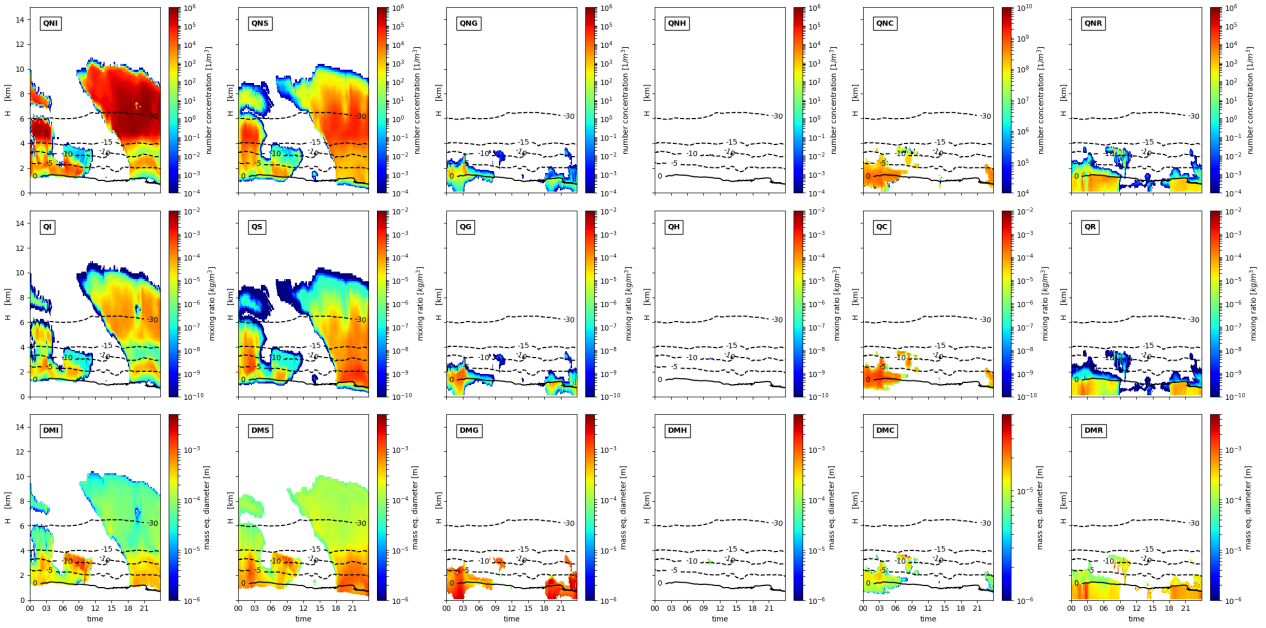

Figure S8. Same as Fig. S1 but for the “needMix2_Akernel" run.

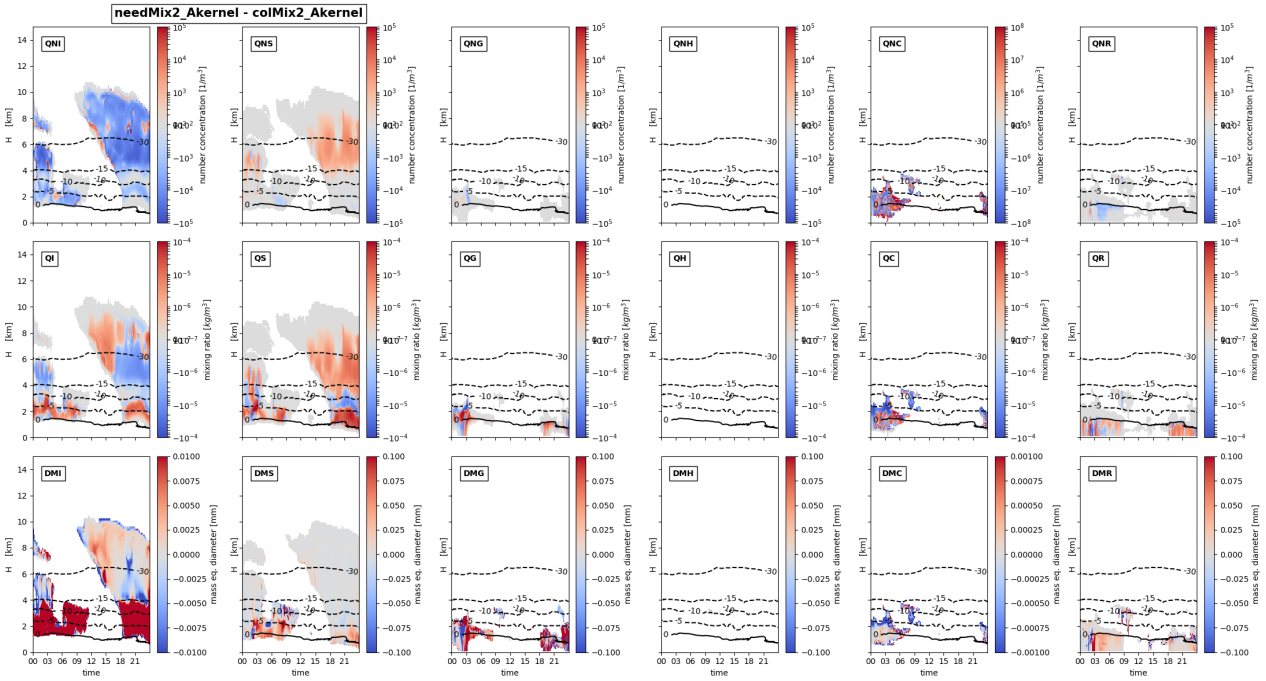

Figure S9. Difference of the hydrometers (same panels as in Fig. S1) between the the “needMix2_Akernel" and the “colMix2_Akernel" (“NEW") run.

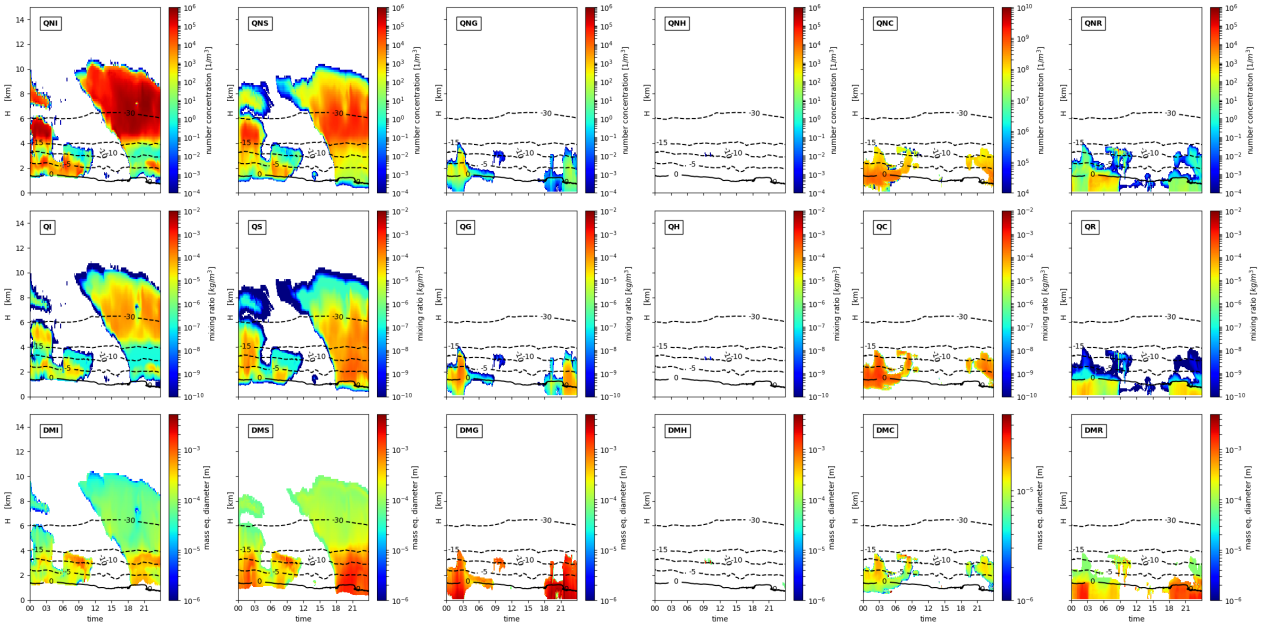

Figure S10. Same as Fig. S1 but for the “colMix2_Dkernel" run.

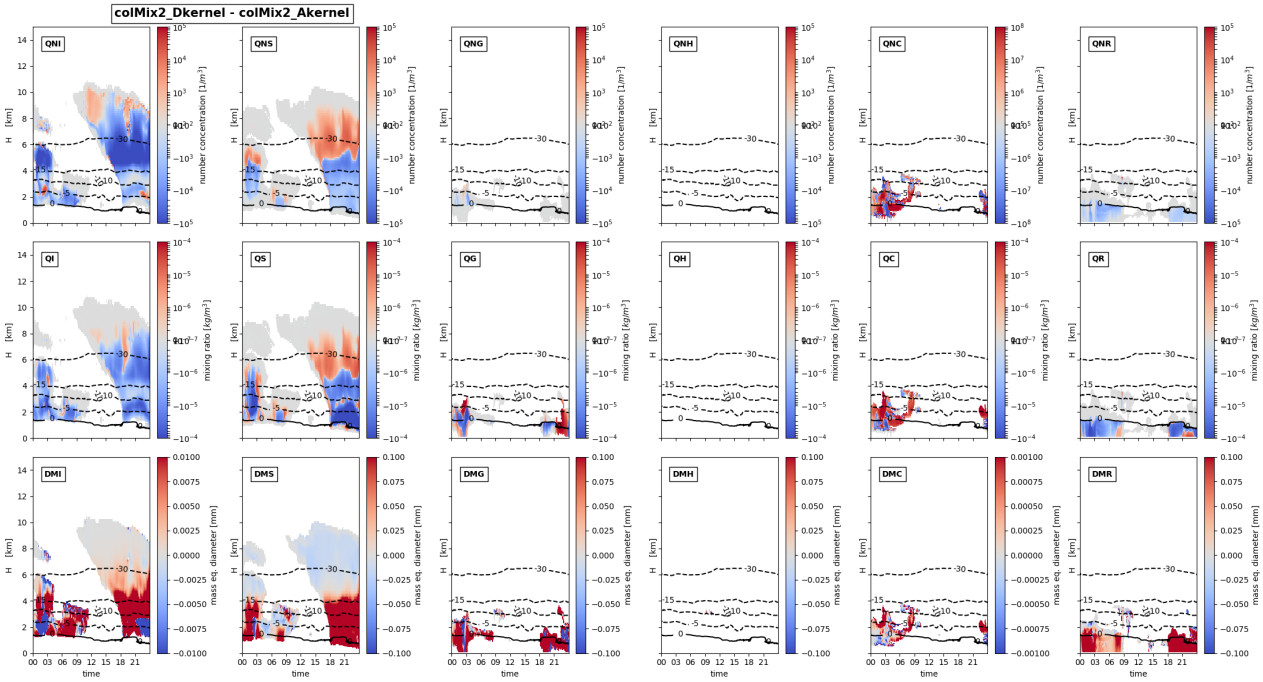

Figure S11. Difference of the hydrometers (same panels as in Fig. S1) between the the “colMix2_Dkernel" and the “colMix2_Akernel" (“NEW") run.

The raindrop size is strongly connected to the size of the snow above, clearly seen by comparing $\mathrm{DWR}_{X,Ka}$ (Fig. 9 in the main text) of the snow with $\mathrm{DWR}_{Ka,W}$ of the rain. While the raindrop size is overestimated in default and “colMix2_Dkernel", where also the size of snow above is overestimated, the raindrop size is fairly matched in the other simulations.

CFTDs Including All profiles

The quantiles and deciles of the observed distributions of DWRs indicate a strong increase in particle size around -15 °C (most evident in $\mathrm{DWR}_{Ka,W}$) and close to the melting layer (most evident in $\mathrm{DWR}_{X,Ka}$; Fig. S13), as also seen in the raining profiles (Fig. 11 in main text). Both of these characteristic increases of the particle sizes can be found in some way in the default and the new simulation (“colMix2_Akernel"). However, the new simulations show a more gentle increase of $DWR_{Ka,W}$ which is more similar to observations (most evident in the upper deciles). Also the increase close to the melting layer in $DWR_{X,Ka}$ better matches the observed profile. The upper decile of $\mathrm{DWR}_{Ka,W}$ reaches 5dB at -8 °C in the SB06 default setup at -12 °C in the new setup and at -10 °C in the observations. The upper decile of $\mathrm{DWR}_{X,Ka}$ increases very rapidly in the default simulation above -7 °C and more slowly in the new simulation and the observation. The increase in lower quantiles of the distribution of both $\mathrm{DWR}_{Ka,W}$ and $\mathrm{DWR}_{X,Ka}$ is relatively similar among simulations and observations.

As in the histogram of the raining profiles (Fig. 12), the overestimation of MDV is also present in the whole temperature range when analyzing all profiles (Fig. S14). Also in this case the overestimation can be attributed to the v_{term}-size relationship

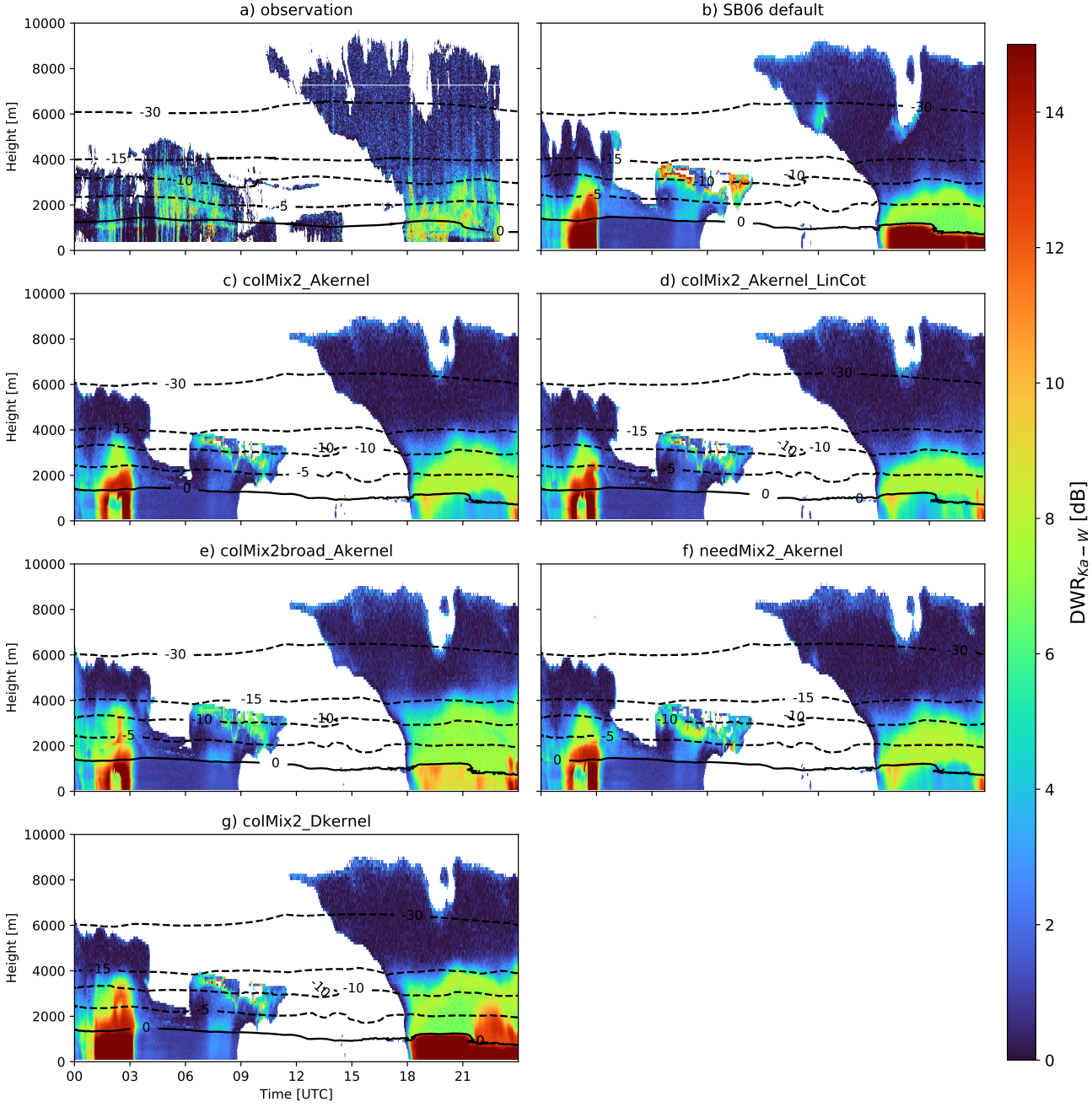

Figure S12. Same as Fig. 8 in main text but displaying the dual-wavelength ratio between Ka- and W-Band ($DWR_{Ka,W}$), which is strongly linked to the particle size.

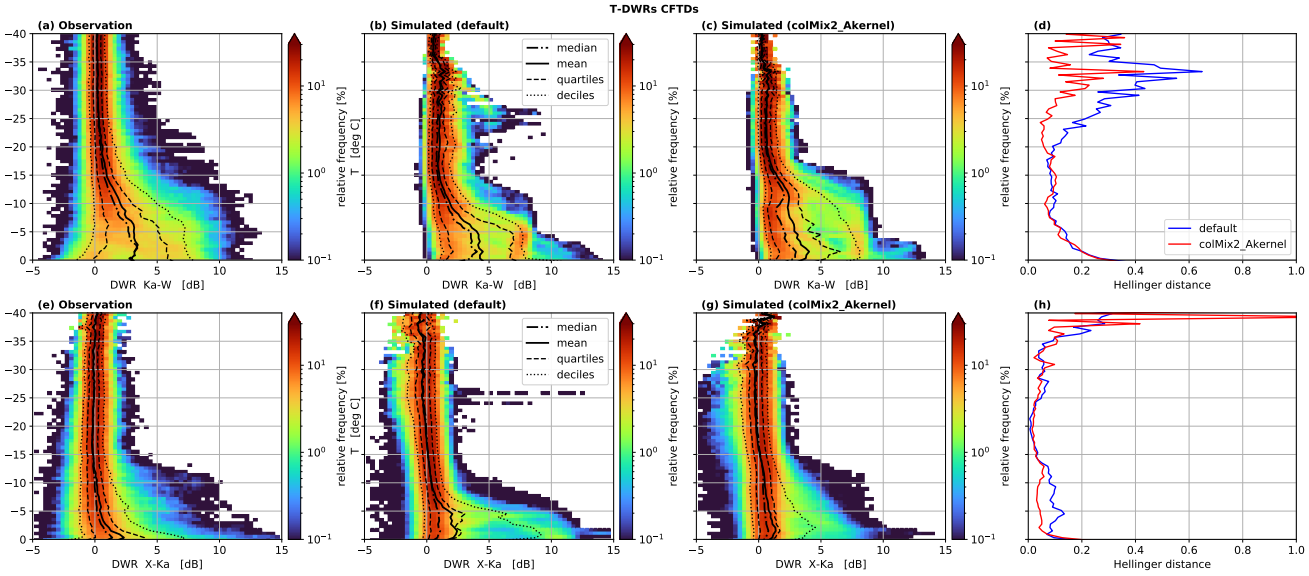

Figure S13. Same as Fig. 11 in main text but taking all profiles and apply no limit on RR.

of the snow class as reported in Karrer et al. (2020). The sharp increase of MDV at temperatures below -35 °C results from the rapid conversion from cloud ice to snow and the large difference between the velocity-size relationship of ice and snow. This rapid increase is not visible in the new model as cloud ice and snow have similar velocities at small sizes. The new simulations reveal considerably lower values of MDV, which fit better to the observations. The mean of MDV reaches 0.75 m/s at -37 °C in the default simulation, at -16 °C in the new simulation, and -20 °C in the observations when considering all profiles (Fig. S14 a to c). The Hellinger distance between the distributions of the new simulation and the observations is smaller for temperatures below -9 °C but larger for higher temperatures. For T$> -9°$ the median of MDV is underestimated by up to 0.4 m/s in the new simulation. As discussed in the analysis of the case study (Sect. 3.4 in the main text) this underestimation is most likely not due to an underestimation of the v_{term} of large aggregates, but due to other processes (e.g. riming, vertical air motion).

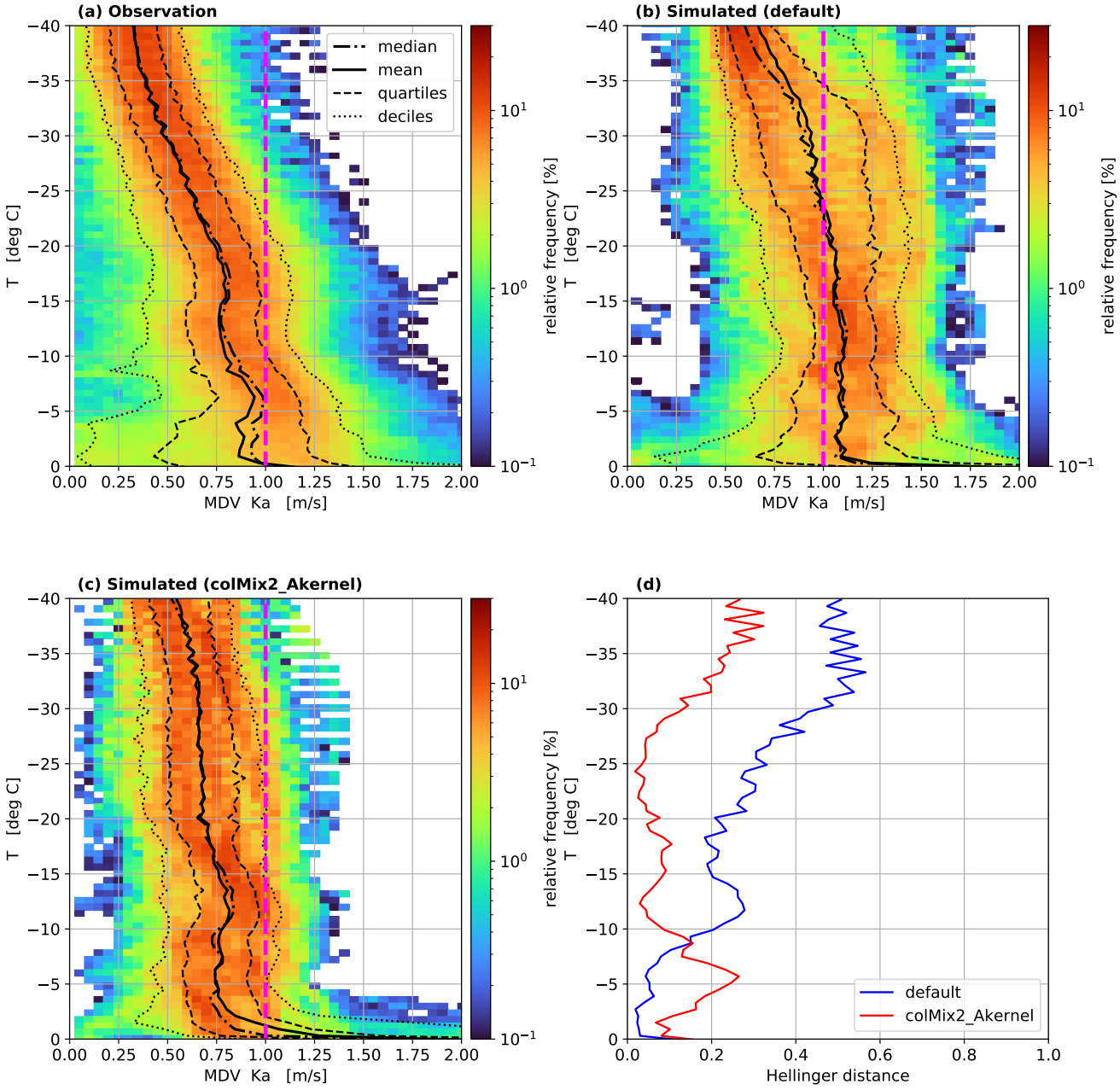

Figure S14. Same as Fig. 12 in main text but taking all profiles and apply no limit on RR.

References

Karrer, M., Seifert, A., Siewert, C., Ori, D., Lerber, A., and Kneifel, S.: Ice Particle Properties Inferred from Aggregation Modelling, Journal of Advances in Modeling Earth Systems, https://doi.org/10.1029/2020ms002066, 2020.